Structural analysis of a newly proposed hybrid wave energy convertor using OpenFOAM

Mobin Masoomi[*1], kourosh Rezanejad[2]

[*1] Department of Mechanical Engineering, Babol Noshirvani University of Technology, Babol, Iran.
[2]Centre for Marine Technology and Ocean Engineering (CENTEC), Instituto Superior Técnico, Universidade de Lisboa, Av. Rovisco Pais, 1049-001, Lisboa, Portugal

Abstract

Fixed Oscillating Water Column (OWC) and Wavestar Wave Energy Converter (WEC) are two standard converters with different strategies but the same goal, extracting energy from waves. Fixed-OWC is a coastal system that uses pneumatic pressure with a turbine, but Wavestar uses a power take-off (PTO) damping system to extract power and operate in both shore and offshore areas. The innovation of the present study is using these two systems simultaneously in a shared platform, in the sense that fixed-OWC is used as the base structure for Wavestar convertor. For this purpose, three main designs with variable distances between the Wavestars' floating object and the fixed-OWCs' front wall, WEC-17.5, WEC-17.8, and WEC-18.1, were performed for four different wavelengths using the numerical solution. The solver is OverInterDymFoam from the standard library of the OpenFOAM solvers, considering both dynamic mesh (Overset mesh technique) and wave generation schemes. Although the idle combination is extracting power from Wavestar besides no efficiency reduction for fixed-OWC, a decrease in efficiency for some cases is inevitable. An overall assessment of the proposed combined system for 12 different case studies reveals that there is an efficiency reduction in some cases, near 38% for the worst case. Still, the superiority of this method is efficiency increment up to 13% for system design points "the efficient span in which the convertor works." Finally, a structural analysis was performed to calculate the exerted force on the front wall of fixed-OWC in the new combined platform.

Keywords: Oscillating water column (OWC); Wavestar; hybrid WEC; OpenFOAM; structural forces.

1. Introduction

We are facing an ever-increasing demand for renewable energy research and development. Ocean energy has proven to be a reliable source of renewable energy and has consequently been subject to various investigations in recent years. The present paper has been introduced the combination of the two types of WEC in a new hybrid installation plan. Here a novel configuration is proposed to use the structure of a fixed-OWC as the base structure for Wavestar[1] WEC. There is no need to build a new fixed structure to install the Wavestar by using this layout, which caused lowering the budget and complexity of the wave energy farm at shorelines. Although some researchers investigated improving the fixed-OWC efficiency, such as using multi-chambers (Shalby et al., 2019) and L-shaped duct (Rezanejad et al., 2019), the purpose of the present study is only to investigate the rate of change in OWC efficiency by adding Wavestar in the front of it. If the OWC's efficiency does not change, our research plan is compelling enough, and whatever the efficiency increases, it is considered an optimal state. The OWC's efficiency is directly related to the free surface motion, chamber pressure, and the phase difference; thus, adding a floated body will probably cause changes in the converter's efficiency.

To the best of the authors' knowledge, similar research has not been performed in the literature. But among various WECs, the fixed-OWC and oscillating buoy prototypes such as the Wavestar have received particular attention (see, e.g., (Falcão & Henriques, 2016), (Drew et al., 2009), (Sarlak et al., 2010)). (Maeda et al., 1985) introduced a simple method to predict the rate of wave energy absorption, a full-scale investigation performed by Takahashi et al. (1993), to improve wave energy converter performance. In addition to shape and type of convertor, some researchers like (Rezanejad et al., 2013) researched the step-bottom for a fixed-OWC numerically; they concluded that adding step-bottom could increase the overall convertors' efficiency. And also,

[1]http://wavestarenergy.com/projects

Ashlin et al. (Ashlin et al., 2016) investigated how the different bottom profile shapes of a nearshore OWC could change the system efficiency. Recently using sequential chambers was an exciting subject for the researchers (Ashlin et al., 2018) installed an array of OWC with different distances to evaluate the total efficiency. Besides, wave frequency is an essential factor in the converter's performance. (Ning et al., 2018) investigated two single and dual-chamber fixed-OWC; they concluded that dual-chamber OWC was more stable, especially for the high-frequency waves. A complete comparison between single and dual-chamber OWC was performed by (Elhanafi et al., 2018). It shows a significant increase in converters' efficiency, about 40% for dual-chamber.

Further, the fixed-WECs, floating structures are other kinds of WEC used both for nearshore and offshore, with different strategies and a wide range of size, water depth, mooring system. The present study combines the floating WEC named Wavestar, which is appropriate with our proposed hybrid system. A scaled model of the Wavestar was investigated by (Jakobsen et al., 2016). After them, (Ransley et al., 2017) analyzed the dynamic behavior of the floated body in fixed and unrestricted (free movement) modes. (Xu et al., 2019) investigated a kind of floating WEC named floating point absorber. They compared the numerical and experimental survival and operational status results and concluded that the most significant discrepancy belonged to surge and pitch RAOs in survivability cases. A 1/5 scale model of Wavestar was investigated by (Windt et al., 2020); they compared the numerical and physical results for all hydrodynamic parameters and related dynamic motions. Besides, they investigated the Froude and Reynolds scaling factors. Recently, they analyzed a Wavestar in operational status to assess the scaling effect on the hydrodynamic parameters and WEC response by considering the numerical solution (Windt et al., 2021). Their conclusion was apart from the mechanical scaling effect, especially friction, numerical modeling in the Numerical Wave Tank (NWT) could accurately model the WEC devices with high fidelity.

Some researchers investigate the hybrid floating WEC, mostly involved installing the converters on floating wind turbine, (Stansby et al., 2022) proposed a wave diffraction radiation model for a floated WEC installed on the floating wind turbine platform. They concluded that the diffraction effects are less than 5%. (Sakr et al., 2021) investigate on controlling the floating WEC to maximize the power absorption; their control system was based on effective stiffness to maintain the natural system frequency near the frequency of the incident wave to have resonance oscillations. (Moreno & Stansby, 2019) experimentally investigate a six-float WEC system with two PTOs installed on the floating wind turbine base structures.

This report addressed extending research based on the previous work by (Masoomi et al., 2021) by considering the three different installation plans of the proposed hybrid system at various wave frequencies to check the comprehensiveness of the investigation. The numerical solution for the new hybrid plan is based on Reynolds Navier Stokes Equation (RANS) by implementing an adjustable NWT, "length in each case study is related to used wave frequency." The OverSetMesh[2] technique, one of the functional new dynamic methods, is used as a dynamic approach on the standard OpenFOAM's[3] solver, "OverInterDyMFoam."

2. Material and Methods

2.1 Governing Equations

The first step in implementing an NWT for wave generating is that the accuracy of this solution is highly dependent on the numerical modeling approach. For instance, the solution based on the potential flow is a low computational cost method appropriate for parametric studies (Penalba et al., 2017; Tanizawa, 2000). High-fidelity but costly methods such as the CFD-based-NWT could accurately track the wave breaking, complex free surface, and turbulence effects. For the present study, an open-source C^{++} The solver "OpenFOAM" uses the RANS equation. A two-phase problem, Air and Water, forcing us to use the Volume Of Fluid (VOF) technique (Nichols et al., 1981) and related boundary and initial conditions. The wave generation and absorption, an integral part of each NWT, are added to the standard solver. Air and water inside the NWT are considered incompressible, and the fluid is Newtonian. The RANS equation, including the continuity and momentum conservation equation (Weller et al., 1998) as described below:

---

[2] https://www.openfoam.com/documentation/guides/latest/doc/guide-overset.html

[3] https://www.openfoam.com

$$\nabla.u = 0 \tag{1}$$

$$\frac{\partial(\rho\,u)}{\partial t} + \nabla.(\rho\,uu) = -\nabla p + \nabla.(\nu\nabla u) + \rho f_b \tag{2}$$

where, u is the fluid velocity, p represents the fluid pressure, ρ, ν are the fluid density and the kinematic viscosity, respectively. f_b denotes the external forces involved gravity, per unit mass. The partial differential equations discretize into the algebraic equation by implementing the Finite Volume Method (FVM). Now it is time to solve these Algebraic equations systems with our three choices, pressure-linked equations (SIMPLE), the pressure-implicit split-operator (PISO), and finally, the combination of these two methods known as PIMPLE. PISO and PIMPLE could be used for transient case studies, whereas the SIMPLE implemented for steady-state problems. The PIMPLE algorithm is considered as an appropriate approach for high-fidelity pressure and velocity coupling. The two-phase flow capturing with the complex free surface is implemented using the VOF technique (Weller et al., 1998).

$$\frac{\partial\alpha}{\partial t} + \nabla.(u\,\alpha) + \nabla.[u_r\,\alpha(1-\alpha)] = 0 \tag{3}$$

$$\rho = \alpha\rho_{water} + (1-\alpha)\rho_{air}, \mu = \alpha\mu_{water} + (1-\alpha)\mu_{air} \tag{4}$$

$$u_r = \min[c_r\,|u|, \max(|u|)] \tag{5}$$

Where α is the phase fraction, $0 < \alpha < 1$, α= 0 denotes water and α= 1 is water. ρ, μ are the density and viscosity respectively, and u_r is the compression velocity. C_r is the factor that controls the interface compression.

2.2 Model Geometry and boundary condition

The first step is devoting an appropriate Numerical Wave Tank (NWT) depending on the type and dimensions of the wave besides considering the solver types, dynamic or static. In this section, the fixed OWC must be validated with the experimental results; the convertors' overall dimensions are included in Table 1. This case is compatible with (Kamath et al., 2015) study; the length of an NWT is usually considered five times the wavelength. The overall domain height is not related to incident wave characteristics and is considered h = 2 m constantly for all cases. The boundary condition is a critical factor that must be following the requirements of each problem. For the wave generating cases, the inlet patch must generate the wave, and the outlet patch is such that the water particles exit without backward current and the atmosphere is total pressure-inlet/outlet; for WEC hull, a no-slip boundary condition is dedicated.

Table.1 The numerical wave tank and the fixed-OWC related dimentions

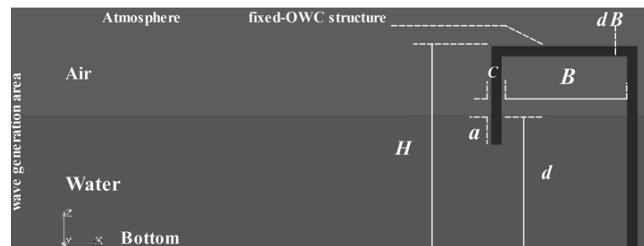| Dimensions [m]	Symbol	Model
OWC- height	H	1.275
OWC thickness	C	0.05
Chamber breadth	B	0.64
Chamber lip height	a	0.15
Orifice width	dB	0.005
Water depth	d	0.92

Fig. 1 The schematic view of the main fixed-OWC dimensions

Needless to say that the first and the main section of this research is producing waves in NWT to test the WECs'. There were some different approaches used before to handle this issue in OpenFOAM. Some extensions could be added to standard solvers such as IHFoam (Higuera et al., 2013a, 2013b, 2014), OlaFoam (Lee et al., 2016; Lee et al., 2017), Wave2Foam (Jacobsen et al., 2015; Lin et al., 2017); furthermore, the waves could generate the same as real wave tanks by using oscillating flaps. For the latest versions of OpenFOAM (version 5.0 onwards), wave generation could be easily accessible with the standard solver "InterFoam." A "waveDict" folder involving the wave parameters was added to the "constant" folder. This solver uses the control volume method to discretize the transport equations, besides the free surface generation, by considering the Volume Of Fluid (VOF) method. Another important factor for wave generation in the NWTs' is the boundary condition, which should be defined as one Inlet and one Outlet. The generated wave from the Inlet boundary condition should exit from the outlet without any back-flow into the domain; (Sommerfeld, 1964) first proposed this kind of boundary condition. In experimental tests, physical beaches, obstacles, friction mechanisms, or sponge layers are used instead.

3. Introducing the Hybrid WEC

The overall objective of this research plan included using a Wavestar energy convertor in front of a fixed-OWC; the only reason for this plan is to use the fixed structure of the OWC as a base structure for the Wavestar device without losing efficiency. The Wavestar was installed in the front of OWC at three different points, as shown in Figure 2, to evaluate the OWC efficiency. The efficiency of the Wavestar is only related to the stroke of the floated body; thus, it is almost constant. In fact, the efficiency of the OWC is complex and related to many factors such as free surface velocity and pressure within the chamber and, more importantly, the phase difference between them. The idle result for this research plan is the efficiency increase; although it could be a plus award, constant efficiency is also considered optimal for the design purpose. But the decrease in efficiency is a drawback of the project. Three different layouts are introduced with the same mechanism; the difference is the distance between the floated-body relative to the front wall of fixed-OWC. Three cases are WEC-17.5, 17.8, 18.1 with the distance of Lx = 0.8, 0.5, 0.2 m from the floated-body center to the front wall of the fixed-OWC.
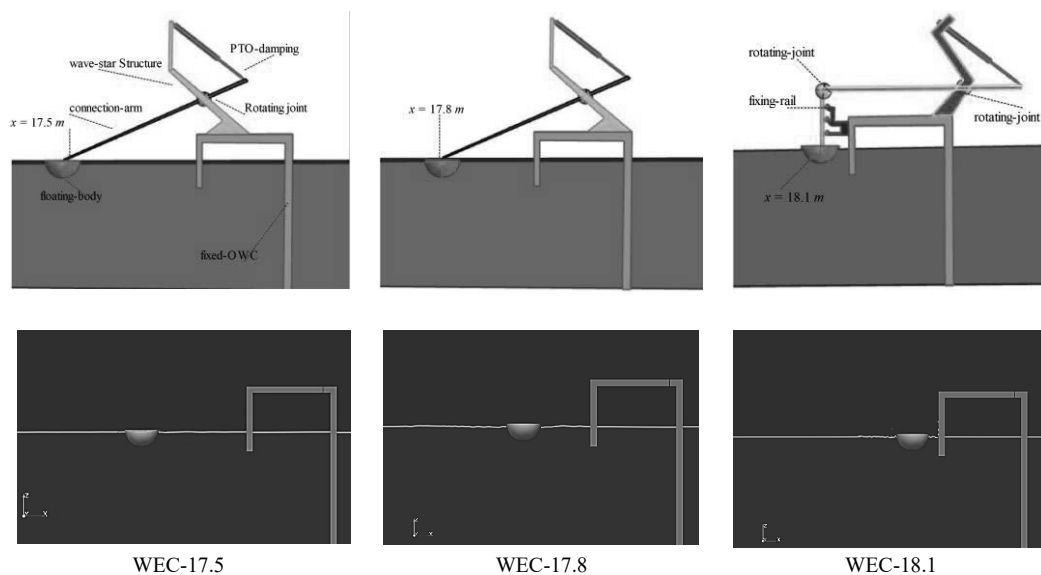

| WEC-17.5 | WEC-17.8 | WEC-18.1 |

Fig. 2 Three different layouts for hybrid system (Wavestar and fixed-OWC combination).

The optimum situation for the new combined system is extracting the same power for OWC with Wavestar rather than the solitary fixed-OWC. However, increasing the power range of the OWC could be impressive; only the same power as before could be enough to prove the efficiency of the new hybrid system. In fact, the purpose of designing this system is not to increase the fixed-OWC efficiency; it is only involved a newly installed Wavestar within the fixed-OWC for further power extraction besides maintaining the former fixed-OWC efficiency. As

mentioned, three main parameters influenced the rate of the output power of OWC, chamber pressure, free surface velocity within the chamber, and the phase difference between pressure and free surface velocity.

3.1 dynamic motions of floating-body

Although the power absorbed by the Wavestar is not considered in the present study, the analysis of the floated semi-hemisphere could be helpful for better understanding and inference. Figure 3 helps us capture the induced motion from generated waves and the water reflection from the fixed-OWC, besides understanding the effect of floated-body distance (x = 17.5, 17.8, 18.1) on the oscillating motions. The standard theoretical motion of the body should be between z = 0.86 and z = 0.98 (initial free surface level: z = 0.92 meter, wave height h = 0.06 meter). As predicted, the reflected waves from fixed-OWC disrupt the floated-body oscillation in both harmony and value such that the worst condition is related to WEC-17.5, the reflected waves combined with the incident wave and decrease the wave efficiency, the situation for WEC-17.8 is better. The idle condition belongs to WEC-18.1, in which the reflected waves could not influence the floated body. Even in the case kd = 0.52 (maximum wave frequency) due to water rise-up on the front wall of the OWC, the top point of the floated-body reaches z = 1.03, which is higher than the theoretical value (z = 0.98). In fact, the lower the wave frequency, the more regular the oscillation of the body and nearer to theoretical values.
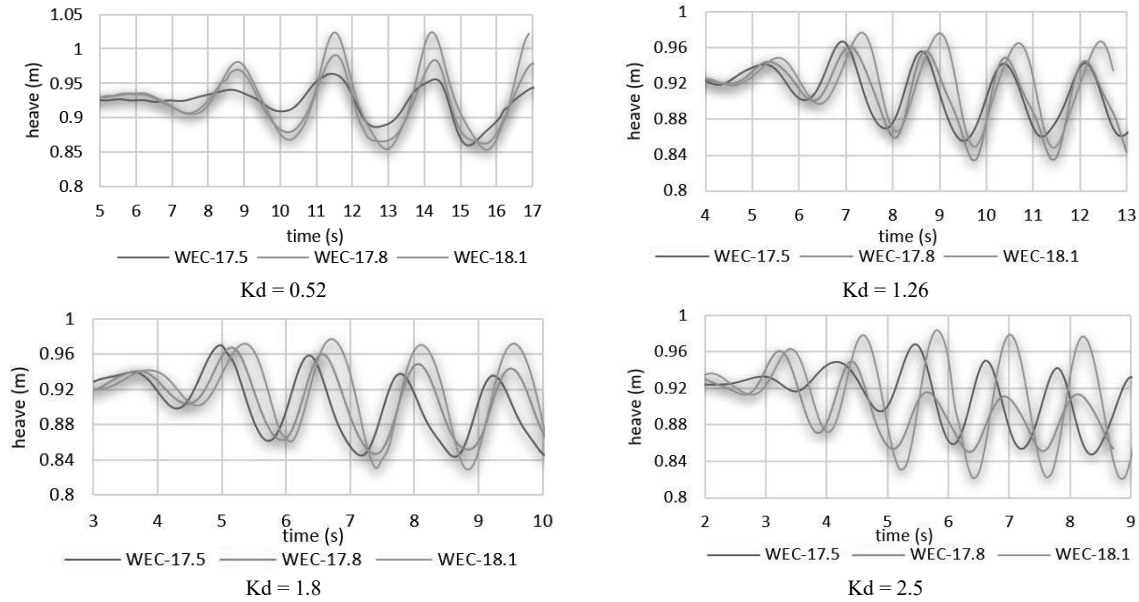

Fig. 3 The heave amplitude of the floated semi-hemisphere for each wavelength

3.2 Total Efficiency Evaluation of the fixed-OWC merged with Wavestar

The efficiency of the WECs with PTO is highly related to the rate of energy flux converted by the device, the inlet energy (P_{in}), Eqs. (6) is the energy of water particles extracted by the fixed-OWC device (P_{out}), Eqs. (7). The share of energy extraction relative to primary energy is called efficiency (η); all these values computes with the following formula:

$$P_{in} = \frac{\rho_w \cdot g \cdot h^2 \cdot \lambda}{16T}\left[1 + \frac{4\pi d/\lambda}{sinh(4\pi d/\lambda)}\right] \tag{6}$$

where h and λ are the wave height and length and d water depth (depth in the OWC chamber),

$$P_{out} = \frac{1}{T}\int_0^T P_c(t) \cdot q(t)dt = \frac{1}{2}|P_c| \cdot |V_{wfs}|b \cdot l \cos(\theta) \tag{7}$$

$$\eta = \frac{P_{out}}{P_{in}} \tag{8}$$

where q(t), (V_{wfs}), (P_c), and (θ) are the volume flow rate, free surface velocity, air pressure, and the phase difference between "(P_c), (V_{wfs})," respectively. As previously mentioned, three parameters affect the fixed-OWC efficiency, chamber pressure (p), free surface velocity (wfs) in the middle of the chamber, and the phase difference between "p" and "wfs." Although these parameters were entirely analyzed in the last sections, a further comparison needs to better understand how these parameters changed when a Wavestar was added to fixed-OWC. A simple way to allocate the percentage value for each parameter is using the disparity symbol, which demonstrates the difference between each new system development rather than standard fixed-OWC.

$$\frac{p_{\text{amended}} - p_{\text{standard}}}{P_{standard}} = \text{disparity}\% \qquad\qquad \frac{e_{\text{amended}} - e_{\text{standard}}}{e_{\text{standard}}} = \text{disparity}\% \qquad (9)$$

The maximum reduction rate of about 40% occurred for kd = 0.52, WEC-17.5, but this value was about 18% for WEC-18.1. These differences show how the position of the floated body could change the results, Figure 4. The device's efficiency has no constant formula; everything goes back to the correlation between wave parameter and fixed-OWC dimension, chamber breath, water depth within the chamber, orifice size, front wall size, etc. Based on all these points, each convertor has its peak efficiency point, kd = 1.26 for the present fixed-OWC. The output's data for "wfs" are quite different, such that the values increased especially in the range of the design point (kd = 1.26 to kd = 1.8), maximum 25% increase for kd = 1.8, WEC-18.1.

Finally, all these values are substituted in the related equation to calculate the total efficiency; the phase difference is considered constant based on our findings, section 3.2.3 only "p" and "wfs" used. For the range of system design points, a slight increase, maximum 12% recorded, Figure 4 is idle for the innovative presented plan. Our optimistic forecast was; no efficiency reduction occurred for the fixed-OWC, and any increment was considered an idle result.
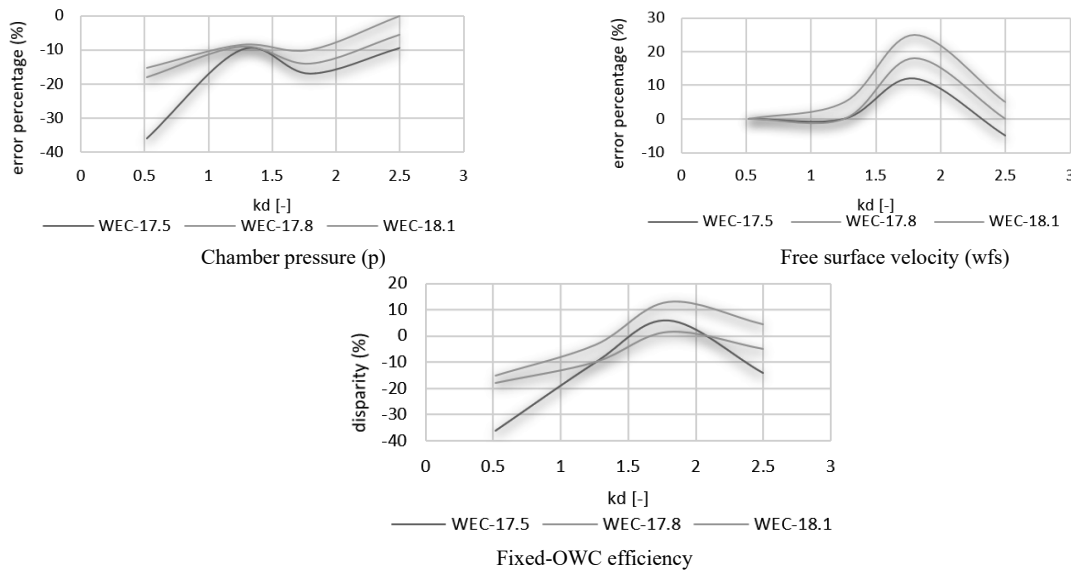

Chamber pressure (p)

Free surface velocity (wfs)

Fixed-OWC efficiency

Fig. 4 Disparity Comparison between the standard model and amended OWC for different wavelengths

3.3 Structural Force

The combination of fixed-OWC and Wavestar could have many challenges, including hydrodynamic and structural issues. The variation of the hydrodynamic efficiency is the most significant issue that should be considered for the present research, but the interpretation of structural loads could be considerable since the front wall of the OWC is the vulnerable part of the convertor which bears the most wave loads on the structure, it is used as a basis for comparison. The durability of a WEC, shore or offshore, is a critical design point that should be considered carefully to prevent system failure. The coastal structure must be constructed so that it can withstand the maximum forces from stormy waves or any harsh conditions. Still, in the present study, only force changes created by adding Wavestar on fixed-OWC will be considered at standard wavelength.

Although the force analysis on the structure is fundamental, little research has been done in this area. (Jayakumar, 1994) investigates induced force on WECs experimentally; (Ashlin et al., 2018; Ashlin et al., 2016) investigate how wave steepness and chamber depth of a fixed-OWC change the indued forces. Wave height is another parameter that greatly impacts the forces acting on the structure, studied by (Didier et al., 2016) with the Smooth Particle Hydrodynamic (SPH) method, especially for the front wall. Further to the standard OWCs, some researchers pay attention to newly introduced fixed-OWC, the hydrodynamic characteristics of a dual-chamber fixed-OWC investigated experimentally by (Ning et al., 2019). (Masoomi et al., 2021) introduced a new design that included adding blades inside the chamber; besides evaluating the hydrodynamic efficiency, a further analysis was performed for the structural force variation due to vertical blades.

In OpenFoam, there are two ways to obtain the forces acting on the structure, first using additional code and library added in controlDict "functionObjectLibs-libforces.so." These are simulation-based solvers; they must be solved simultaneously with the primary simulation in each time step. The second choice is to use the post-processing tool ParaView to capture the point by point pressure, surface, and surface normals and calculate the resulting forces, finally integrating the new defined variable "force" to extract the diagrams. For the case in-hand a normal pressure F_p is considered the basis of comparison, Eqs. (10) calculates any force on the desired section, wave-induced force, hydrostatic force, and air force.

$$F_p = \sum \omega_i \cdot S_{f,i} (p_i - p_{ref})$$
(10)

Where ω_i is the density, $S_{f,i}$ the face area vector, p the pressure. The initial impression is that the shorter the wavelength, the greater the forces acting on the front wall; Figure 5 maximum pressure P = 12 [N], for kd = 0.52 and P = 32 [N] for kd = 2.5. The force variations are the same as the pressure changes, with no constant trend; thus, the force changes are different for kd = 1.26 rather than kd = 2.5. Because for "kd = 1.26, WEC-18.1" force decreased, but for "kd = 2.5, WEC-18.1" the exerted force increased by about 30%, albeit for "kd = 1.26, WEC-17.5" the force reduced to approximately 18%. As we concluded in the last section, WEC-17.5, the pneumatic pressure decreases within the chamber apart from the wave frequency. The condition is also applied for force evaluation such that, for WEC-17.5, the force decreases for all wavelengths.
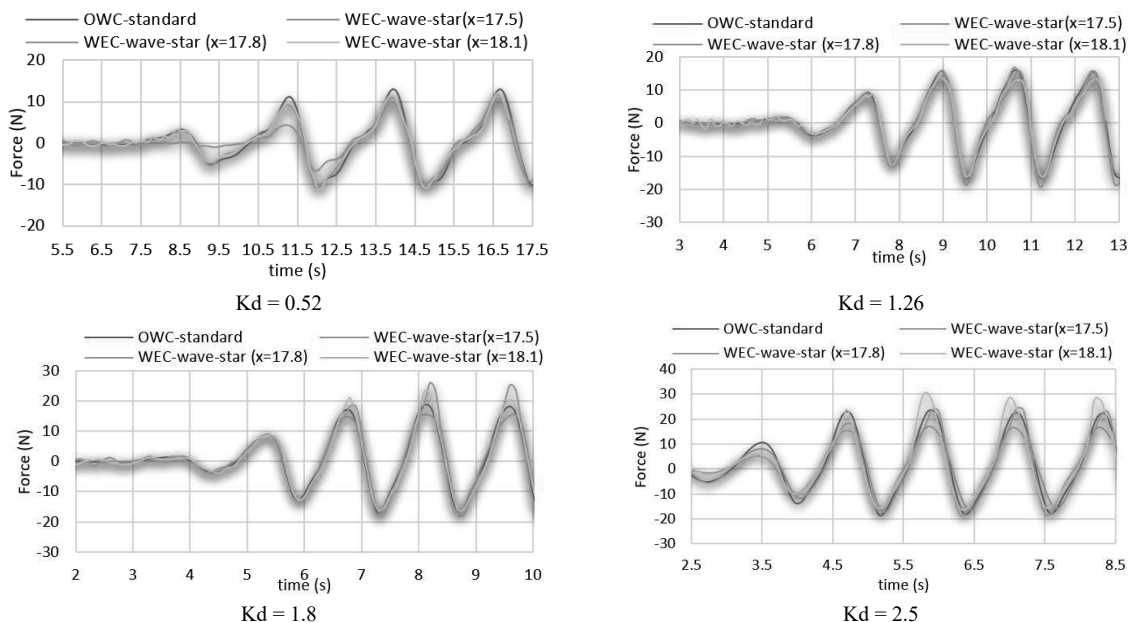

Fig. 5 Horizontal force values acting on a standard OWC for different kd.

To better understand why WEC-18.1 increases the wave exerted forces? The answer is represented by a contour-based figure designated for three different combination layouts for kd = 2.5; the reason for using kd = 2.5 is; it had changed a lot. It is all about cumulative pressure beneath the floated body and the front wall of the fixed-

OWC. As the floated body is installed closer to the front wall, the entrapped water gains more energy; this extra energy increases the pressure, resulting in the structural force. This could easily be inferred based on the pressure contour in Fiure 6. The pressure is shown between p = 8000 [pa] and p = 11000 [pa]; the cumulative pressure is quite obvious for WEC-17.8 and WEC-18.1. These regional pressures only influenced the structural forces, and there were not many obvious differences observed for the chamber's pressure.
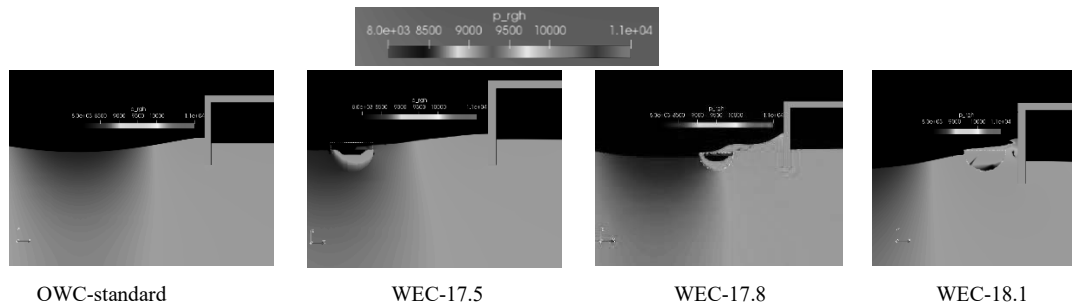

OWC-standard   WEC-17.5   WEC-17.8   WEC-18.1

Fig. 6 Pressure contour for the different hybrid plan, WEC-17.5, 17.8, 18.1 versus standard fixed-OWC for kd= 2.5.

4. Conclusions

Increasing demand for green energy induces the need for a more efficient renewable energy source with lower complexity, and structural cost spread rapidly worldwide. In the present study, we proposed a simple but efficient way to decrease the structural costs by combining two different wave energy convertors, fixed-OWC, and Wavestar, in a shared platform. The hybrid WEC system was designed based on the different installed positions of floated-body in the front of fixed-OWC, WEC-17.5, 17.8, 18.1. Since each convertor has its system design point and related efficiency, Due to incident wavelength and the converters' dimension, especially chamber breath, the proposed hybrid WEC, investigated with the most important work condition (system design point, kd = 1.26 for the present fixed-OWC). The simulated wave number for the three case studies was kd = 0.52, 1.26, 1.8, 2.5. The structural loads were investigated based on the hydrodynamic pressures. The obtained results were related to only the front wall; WEC-18.1 increased the structural load, near 30% for the worst condition and WEC-17.5 decreased these exerted loads, about 18% for the best condition, the opposite of the efficiency results. Albeit these are logical, due to cumulative pressure between the floated-body and the front wall of the fixed-OWC. Less distance caused less cumulative pressure and consequently less structural force; therefore, WEC-18.1 with dx = 0.2 meters applied more loads than WEC-17.5 with dx = 0.8-meter distance.

Nomenclature Latin letters

a	Chamber lip height [m]		
B	Chamber breadth [m]	wfs	Free surface velocity [m.s^{-1}]
C	OWC thickness [m]	kd	Wavenumber [-]
d	Water depth [m]	dB	Orifice width [m]
E	error [%]	X	Position vector [m]
e	efficiency value [%]	T	Wave period [s]
EL	Free surfce elevation	U	Velocity vector [m.s^{-1}]
g	Acceleration of gravity [m.s^{-2}]	h	Wave height [m]
F	Force [N]	k	Angular Wavenumber [m^{-1}]
b	Sub-chamber width [m]	Z	Height of plates [m]
H	OWC height [m]		

Greek letters

λ	Wave length [m]	ε	Kinetic energy dissapation rate
ν	Fluid kinematic viscosity	ω	Angular frequency

τ_{ij}	Reynolds Stress term	θ	Phase difference
κ	Turbulent Kinetic energy	η	efficiency symbol
ρ	Density [kg.m⁻³]	ζ	Wave steepness [-]

References

Ashlin, S. J., Sannasiraj, S., & Sundar, V. (2018). Performance of an array of oscillating water column devices integrated with an offshore detached breakwater. *Ocean Engineering, 163*, 518-532.

Ashlin, S. J., Sundar, V., & Sannasiraj, S. (2016). Effects of bottom profile of an oscillating water column device on its hydrodynamic characteristics. *Renewable energy, 96*, 341-353.

Didier, E., Neves, D. R., Teixeira, P. R., Dias, J., & Neves, M. G. (2016). Smoothed particle hydrodynamics numerical model for modeling an oscillating water chamber. *Ocean Engineering, 123*, 397-410.

Elhanafi, A., Macfarlane, G., & Ning, D. (2018). Hydrodynamic performance of single–chamber and dual–chamber offshore–stationary Oscillating Water Column devices using CFD. *Applied Energy, 228*, 82-96.

Falcão, A. F., & Henriques, J. C. (2016). Oscillating-water-column wave energy converters and air turbines: A review. *Renewable energy, 85*, 1391-1424.

Higuera, P., Lara, J. L., & Losada, I. J. (2013a). Realistic wave generation and active wave absorption for Navier–Stokes models: Application to OpenFOAM®. *Coastal Engineering, 71*, 102-118.

Higuera, P., Lara, J. L., & Losada, I. J. (2013b). Simulating coastal engineering processes with OpenFOAM®. *Coastal Engineering, 71*, 119-134.

Higuera, P., Lara, J. L., & Losada, I. J. (2014). Three-dimensional interaction of waves and porous coastal structures using OpenFOAM®. Part II: Application. *Coastal Engineering, 83*, 259-270.

Jacobsen, N. G., van Gent, M. R., & Wolters, G. (2015). Numerical analysis of the interaction of irregular waves with two dimensional permeable coastal structures. *Coastal Engineering, 102*, 13-29.

Jakobsen, M. M., Beatty, S., Iglesias, G., & Kramer, M. M. (2016). Characterization of loads on a hemispherical point absorber wave energy converter. *International Journal of Marine Energy, 13*, 1-15.

Jayakumar, V. (1994). *Wave force on oscillating water column type wave energy caisson: an experiment study* Ph. D. thesis, Dept. of Ocean Engineering, Indian Institute of Technology].

Kamath, A., Bihs, H., & Arntsen, Ø. A. (2015). Numerical investigations of the hydrodynamics of an oscillating water column device. *Ocean Engineering, 102*, 40-50.

Lee, K.-H., Bae, J.-H., An, S.-W., Kim, D.-S., & Bae, K. S. (2016). Numerical analysis on wave characteristics around submerged breakwater in wave and current coexisting field by OLAFOAM. *Journal of Korean Society of Coastal and Ocean Engineers, 28*(6), 332-349.

Lee, K.-H., Bae, J.-H., Kim, S.-G., & Kim, D.-S. (2017). Three-dimensional simulation of wave reflection and pressure acting on circular perforated caisson breakwater by OLAFOAM. *Journal of Korean Society of Coastal and Ocean Engineers, 29*(6), 286-304.

Lin, Z., Pokrajac, D., Guo, Y., Jeng, D.-s., Tang, T., Rey, N., Zheng, J., & Zhang, J. (2017). Investigation of nonlinear wave-induced seabed response around mono-pile foundation. *Coastal Engineering, 121*, 197-211.

Lopez Mejia, O. D., Mejia, O. E., Escorcia, K. M., Suarez, F., & Laín, S. (2021). Comparison of Sliding and Overset Mesh Techniques in the Simulation of a Vertical Axis Turbine for Hydrokinetic Applications. *Processes, 9*(11), 1933.

Maeda, H., Kinoshita, T., Masuda, K., & Kato, W. (1985). Fundamental research on oscillating water column wave power absorbers.

Masoomi, M., & Mosavi, A. (2021). The One-Way FSI Method Based on RANS-FEM for the Open Water Test of a Marine Propeller at the Different Loading Conditions. *Journal of Marine Science and Engineering, 9*(4), 351.

Masoomi, M., Yousefifard, M., & Mosavi, A. (2021). Efficiency Assessment of an Amended Oscillating Water Column Using OpenFOAM. *Sustainability, 13*(10), 5633.

Moreno, E. C., & Stansby, P. (2019). The 6-float wave energy converter M4: Ocean basin tests giving capture width, response and energy yield for several sites. *Renewable and Sustainable Energy Reviews, 104*, 307-318.

Nichols, B., Hirt, C., & Hotchkiss, R. (1981). Volume of fluid (VOF) method for the dynamics of free boundaries. *Journal of Computational Physics, 39*(1), 201-225.

Ning, D.-z., Wang, R.-q., Chen, L.-f., & Sun, K. (2019). Experimental investigation of a land-based dual-chamber OWC wave energy converter. *Renewable and Sustainable Energy Reviews, 105*, 48-60.

Ning, D., Zhou, Y., & Zhang, C. (2018). Hydrodynamic modeling of a novel dual-chamber OWC wave energy converter. *Applied Ocean Research, 78*, 180-191.

Nuernberg, M., & Tao, L. (2018). Three dimensional tidal turbine array simulations using OpenFOAM with dynamic mesh. *Ocean Engineering, 147*, 629-646.

Penalba, M., Giorgi, G., & Ringwood, J. V. (2017). Mathematical modelling of wave energy converters: A review of nonlinear approaches. *Renewable and Sustainable Energy Reviews, 78*, 1188-1207.

Ransley, E., Greaves, D., Raby, A., Simmonds, D., Jakobsen, M. M., & Kramer, M. (2017). Rans-vof modelling of the wavestar point absorber. *Renewable energy, 109*, 49-65.

Rezanejad, K., Bhattacharjee, J., & Soares, C. G. (2013). Stepped sea bottom effects on the efficiency of nearshore oscillating water column device. *Ocean engineering, 70*, 25-38.

Rezanejad, K., Souto-Iglesias, A., & Soares, C. G. (2019). Experimental investigation on the hydrodynamic performance of an L-shaped duct oscillating water column wave energy converter. *Ocean Engineering, 173*, 388-398.

Sakr, A. H., Metwalli, S. M., & Anis, Y. H. (2021). Dynamics of Heaving Buoy Wave Energy Converters with a Stiffness Reactive Controller. *Energies, 14*(1), 44.

Sarlak, H., Seif, M. S., & Abbaspour, M. (2010). Experimental investigation of offshore wave buoy performance. *Journal of Marine Engineering, 6*(11), 0-0.

Shalby, M., Elhanafi, A., Walker, P., & Dorrell, D. G. (2019). CFD modelling of a small–scale fixed multi–chamber OWC device. *Applied Ocean Research, 88*, 37-47.

Sommerfeld, A. (1964). *Thermodynamics and statistical mechanics* (Vol. 5). CUP Archive.

Stansby, P., Moreno, E. C., Draycott, S., & Stallard, T. (2022). Total wave power absorption by a multi-float wave energy converter and a semi-submersible wind platform with a fast far field model for arrays. *Journal of Ocean Engineering and Marine Energy, 8*(1), 43-63.

Takahashi, S., Nakada, H., Ohneda, H., & Shikamori, M. (1993). Wave power conversion by a prototype wave power extracting caisson in Sakata port. In *Coastal Engineering 1992* (pp. 3440-3453).

Tanizawa, K. (2000). The state of the art on numerical wave tank. Proceedings of 4th Osaka Colloquium on Seakeeping Performance of Ships 2000,

Weller, H. G., Tabor, G., Jasak, H., & Fureby, C. (1998). A tensorial approach to computational continuum mechanics using object-oriented techniques. *Computers in physics, 12*(6), 620-631.

Windt, C., Davidson, J., Ransley, E. J., Greaves, D., Jakobsen, M., Kramer, M., & Ringwood, J. V. (2020). Validation of a CFD-based numerical wave tank model for the power production assessment of the wavestar ocean wave energy converter. *Renewable Energy, 146*, 2499-2516.

Windt, C., Davidson, J., & Ringwood, J. V. (2021). Numerical analysis of the hydrodynamic scaling effects for the Wavestar wave energy converter. *Journal of Fluids and Structures, 105*, 103328.

Xu, Q., Li, Y., Yu, Y.-H., Ding, B., Jiang, Z., Lin, Z., & Cazzolato, B. (2019). Experimental and numerical investigations of a two-body floating-point absorber wave energy converter in regular waves. *Journal of Fluids and Structures, 91*, 102613.